Title

Neuropilin-1 distinguishes natural and inducible regulatory T cells among regulatory T cell subsets in vivo

Journal

Journal of Experimental Medicine, 209(10)

ISSN

0022-1007

Authors

Yadav, Mahesh
Louvet, Cedric
Davini, Dan
et al.

Publication Date

2012-09-24

DOI

10.1084/jem.20120822

Peer reviewed

Neuropilin-1 distinguishes natural and inducible regulatory T cells among regulatory T cell subsets in vivo

Mahesh Yadav,[1] Cedric Louvet,[1] Dan Davini,[1] James M. Gardner,[1,2] Marc Martinez-Llordella,[1] Samantha Bailey-Bucktrout,[1] Bryan A. Anthony,[3] Francis M. Sverdrup,[3] Richard Head,[4] Daniel J. Kuster,[4] Peter Ruminski,[4] David Weiss,[4] David Von Schack,[4] and Jeffrey A. Bluestone[1]

[1]Diabetes Center and [2]Department of Surgery, University of California, San Francisco, San Francisco, CA 94122
[3]Center for World Health & Medicine, Saint Louis University, Saint Louis, MO 63103
[4]Inflammation and Immunology Research Unit, Pfizer Biotherapeutics Research and Development, Cambridge, MA 02140

Foxp3$^+$ CD4$^+$ T helper cells called regulatory T (T reg) cells play a key role in controlling reactivity to self-antigens and onset of autoimmunity. T reg cells either arise in thymus and are called natural T reg (nT reg) cells or are generated in the periphery through induction of Foxp3 and are called inducible T reg (iT reg) cells. The relative contributions of iT reg cells and nT reg cells in peripheral tolerance remain unclear as a result of an inability to separate these two subsets of T reg cells. Using a combination of novel TCR transgenic mice with a defined self-antigen specificity and conventional mouse models, we demonstrate that a cell surface molecule, neuropilin-1 (Nrp-1), is expressed at high levels on nT reg cells and can be used to separate nT reg versus iT reg cells in certain physiological settings. In addition, iT reg cells generated through antigen delivery or converted under homeostatic conditions lack Nrp-1 expression. Nrp-1^{lo} iT reg cells show similar suppressive activity to nT reg cells in controlling ongoing autoimmune responses under homeostatic conditions. In contrast, their activity might be compromised in certain lymphopenic settings. Collectively, our data show that Nrp-1 provides an excellent marker to distinguish distinct T reg subsets and will be useful in studying the role of nT reg versus iT reg cells in different disease settings.

CORRESPONDENCE
Jeffrey A. Bluestone:
Jeff.Bluestone@ucsf.edu

Abbreviations: EAE, experimental autoimmune encephalomyelitis; iT reg cell, inducible T reg cell; MBP, myelin basic protein; NOD, nonobese diabetic; Nrp-1, neuropilin-1; nT reg cell, natural T reg cell; RAG, recombination activation gene; Tg, transgenic; T conv cell, conventional T cell; T reg cell, regulatory T cell; TSDR, T reg cell–specific demethylation region.

Foxp3$^+$ regulatory T (T reg) cells constitute a population of CD4$^+$ T cells that plays a key role in maintaining immune homeostasis and tolerance (Bennett et al., 2001). Foxp3$^+$ T reg cells arise both in the thymus (natural T reg [nT reg] cells) and in the periphery (inducible T reg [iT reg] cells) as a consequence of exposure to antigens (Bluestone and Abbas, 2003). TCR repertoire analysis and intracellular expression of Helios, a member of the ikaros family of transcription factors, suggest that iT reg cells could constitute up to 30% of total T reg cells in the periphery (Hsieh et al., 2004; Pacholczyk et al., 2006; Wong et al., 2007) and may be important in regulating autoimmunity (Feuerer et al., 2010). However, the use of Helios as a marker to distinguish iT reg cells has been controversial as a result of its inconsistent expression on iT reg cells in distinct immune settings (Thornton et al., 2010; Akimova et al., 2011; Gottschalk et al., 2012).

iT reg cells are induced in vivo in several experimental settings including the treatment of mice with minute doses of antigen delivered using osmotic pump or by directing antigen to DEC-205$^+$ dendritic cells (Apostolou and von Boehmer, 2004). Similarly, a study by Mucida et al. (2005) showed that OVA-specific Foxp3$^+$ T reg cells appeared in the gut of mice administered with antigen orally. Importantly, unlike in the in vitro induced cells, in vivo generated iT reg cells exhibited a demethylated Foxp3 T reg cell–specific demethylation region (TSDR; Polansky et al., 2008). Functionally, iT reg cells

C. Louvet's present address is INSERM U1064, Université de Nantes, Nantes 44093, France.

The Rockefeller University Press $30.00
J. Exp. Med. 2012 Vol. 209 No. 10 1713-1722
www.jem.org/cgi/doi/10.1084/jem.20120822

The Journal of Experimental Medicine

have been shown to be protective in some studies (Mottet et al., 2003; Huter et al., 2008; Haribhai et al., 2011) although others have reported less efficacy (Hill et al., 2007). This might be a result of different disease models or the use of in vivo versus in vitro generation of iT reg cells. Thus, the exact contribution of iT reg cells in maintaining peripheral tolerance remains unclear.

In this study, we addressed the phenotype and function of nT reg versus iT reg cells using a newly defined marker, neuropilin-1 (Nrp-1), which was found to be selectively expressed on nT reg cells and not on in vivo or in vitro generated iT reg cells. By separating Foxp3$^+$ T reg cells into Npr-1^{lo} iT reg and Nrp-1^{hi} nT reg cells, we were able to analyze their regulatory functions in suppressing autoimmune responses in vivo.

RESULTS AND DISCUSSION

Spontaneous generation of iT reg cells in myelin basic protein (MBP)–TCR-transgenic (Tg) mouse

In the current study, we took advantage of an MBP-specific TCR-Tg mouse developed in our laboratory to study T reg subsets. The MBP-specific TCR-Tg mouse (1B3) was created by cloning the rearranged TCR-α (Vα5) and -β (Vβ14) chains of a CD4$^+$ T cells from infiltrated peripheral nerves of a nonobese diabetic (NOD) mouse deficient for the co-stimulatory molecule B7-2 (NOD-B7-2KO; Louvet et al., 2009; Fig. S1). 1B3 mice bred onto recombination activation gene (RAG)–deficient background developed a rapid and fatal experimental autoimmune encephalomyelitis (EAE). Examination of Foxp3$^+$ T reg cells showed that NOD.1B3.RAG$^+$ mice expressed T reg cells in the thymus but not when mice were bred onto the RAG-deficient background (Fig. 1 a). Interestingly, a significant number of Foxp3$^+$ T reg cells were observed in the periphery of the RAG-deficient 1B3 mice based on both intracellular staining for Foxp3 and on crossing the 1B3.RAG onto Foxp3-GFP background (Fig. 1 a and not depicted). The Foxp3$^+$CD4$^+$ T cells were completely absent at birth in 1B3.RAG$^{-/-}$ mice and began to emerge only in the periphery (spleen and LN) at ∼3 wk, consistent with the development of these cells outside the thymus. The frequency of T reg cells in 1B3.RAG$^{-/-}$ mice in the periphery reached comparable levels to RAG$^{+/-}$ littermate controls (1B3 and WT) in mice that survived to 6 wk (Fig. 1 b and not depicted). Foxp3$^+$ T reg cells from 1B3.RAG$^{-/-}$ expressed similar levels of canonical T reg markers such as Foxp3, GITR, CTLA-4, and CD25 (Fig. 1 a and not depicted). Together, the data suggest that the T reg cells in IB3.RAG$^{-/-}$ develop in the periphery but not in the thymus. The spontaneous generation of iT reg cells was likely a result of the ubiquitous expression of MBP in the periphery that led to the initial induction of iT reg cells (Voskuhl, 1998). Interestingly, MBP is also expressed in the thymus but T reg cells were not generated. This contrasts with earlier studies using HA-specific TCR Tg mouse, where self-peptide expression in thymus induced thymocytes to differentiate into T reg cells (Larkin et al., 2008). However, recent studies of an insulin-specific TCR Tg mouse demonstrated similar findings to ours, reflecting differences in recognition of distinct natural auto-antigens in the thymus most likely based on TCR affinities (Fousteri et al., 2012).

1B3.RAG$^{-/-}$ T reg cells are generated in periphery

To further confirm that T reg cells in the 1B3.RAG$^{-/-}$ mice were indeed iT reg cells, we compared the development of Foxp3$^+$CD4$^+$ T reg cells in the peripheral lymphoid organs in euthymic versus athymic 1B3.RAG$^{-/-}$ mice. As shown in one representative cohort of five mice, the number of peripheral T reg cells appeared similar in the athymic animals as compared with control (sham-operated) littermates (Fig. 1 c). Next, we injected thymocytes from a 2-wk-old 1B3.RAG$^{-/-}$ into thymuses of congenic WT mice and monitored their T reg development to rule out the possibility that interclonal competition restricted the development of T reg cells in the thymus (Bautista et al., 2009; Leung et al., 2009). As shown in Fig. 1 d, <0.5% of CD4$^+$ single positive 1B3.RAG$^{-/-}$ cells became Foxp3$^+$ after 4 d of transfer in this setting. This is significantly less than the percentage previously reported by Bautista et al. (2009) and Leung et al. (2009) where a 100-fold greater frequency of Foxp3$^+$ cells was detected using the TCR-Tg cells cloned from a Foxp3$^+$ cell TCR. These data strongly suggest that the absence of T reg cells in the thymuses of 1B3.RAG$^{-/-}$ mice was not a result of the interclonal competition.

We also ruled out that the development of iT reg cells in the 1B3 model was a consequence of the inflammatory environment in the RAG-deficient 1B3 background. Radiation bone marrow chimeras were generated by mixing 1B3.RAG$^{-/-}$ bone marrow with congenically marked WT bone marrow (1:1). Foxp3$^+$ T reg cells in the thymus were derived solely from the WT bone marrow, whereas 1B3.RAG$^{-/-}$ bone marrow failed to generate any T reg cells in the thymus. However, there was a significant number of 1B3.RAG$^{-/-}$ bone marrow–derived T reg cells in spleen and LN (Fig. 1 e). Most importantly, the mixed chimeras showed no signs of disease or evidence of autoimmunity (unpublished data), consistent with the conclusion that the iT reg cells develop as a consequence of immune homeostasis and not fulminant autoimmunity.

Nrp-1 is differentially expressed on natural and iT reg cells

To define the transcriptional characteristics and distinctly regulated genes between nT reg and iT reg cells, we compared 1B3.RAG$^{-/-}$ iT reg cells with T reg cells isolated from periphery of WT or 1B3 mice. Approximately 700 transcripts were differentially expressed (at least threefold) between all T reg cells and iT reg cells (fold discovery rate cutoff at 0.01). A more systematic analysis of transcripts showed that a subset of transcripts was selectively expressed at reduced levels in iT reg cells (highlighted in box in Fig. 2 a), which included PD-1 (programmed cell death -1, pdcd1), Nrp-1, Helios (Ikzf2), and CD73 (Nt5e; Fig. 2 b and Fig. S2).

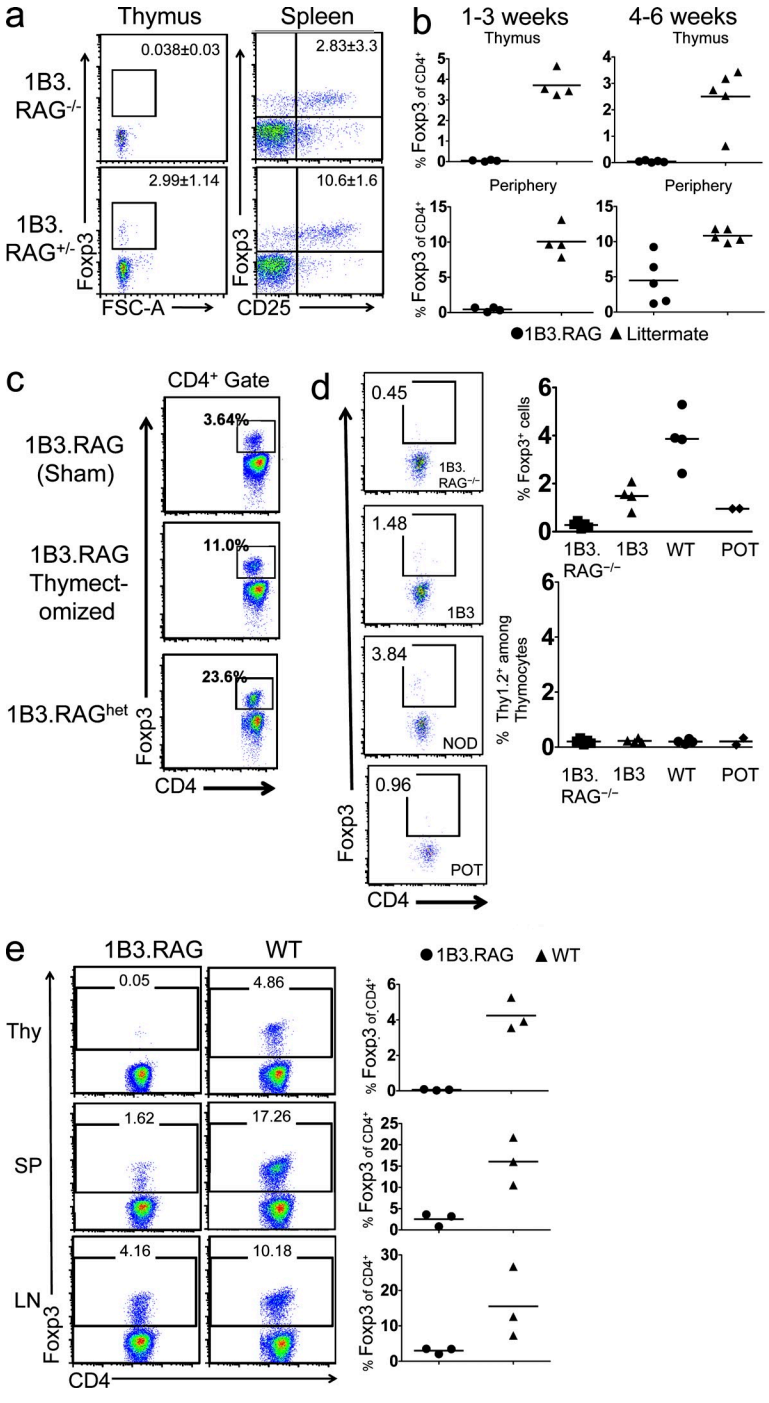

Figure 1. iT reg cells are generated in 1B3.RAG$^{-/-}$ mouse in the periphery. (a) Flow cytometric staining for Foxp3 expression in CD4$^+$CD8$^-$ T cells in the thymus and spleen of 5-wk-old 1B3.RAG$^{-/-}$ (top) or 1B3.RAG$^{+/-}$ littermates (bottom). Numbers indicate mean ± SD of Foxp3$^+$ cells from four individual mice. (b) Foxp3 expression in the CD4$^+$CD8$^-$ T cells from thymus or pooled spleen+LN of 1B3.RAG$^{-/-}$ or 1B3.RAG$^{+/-}$ littermate mice aged 1–3 or 4–6 wk. Each dot represents percentage of Foxp3$^+$ cells from an individual mouse and bars represent means. (c) Foxp3 staining in pooled spleen and LN cells from 3.5–4-wk-old mice thymectomized neonatally. Littermates 1B3.RAG$^{+/-}$ or sham-operated 1B3.RAG$^{-/-}$ mice were used as controls. A single representative mouse out of five thymectomized mice is shown. (d) Foxp3 staining in Thy1.2$^+$ cells in the CD4$^+$CD8$^-$ subset after intrathymic injection of 10^7 thymocytes from 1-wk-old 1B3, 1B3.RAG$^{-/-}$, WT, or POT (P0-specific TCR-Tg) mice into congenic Thy1.1 host, followed by flow cytometry on day 4. A representative plot is shown on the left. On the right are graphs showing the percentage of Foxp3$^+$ cells among CD4$^+$CD8$^-$ cells (top) and percentage of Thy1.2$^+$ cells among total thymocytes (bottom) with bars representing means. Data are representative of two independent experiments. (e) Mixed bone marrow chimeras were generated by mixing (1:1) congenically marked WT and 1B3.RAG$^{-/-}$ bone marrow. 6 wk after reconstitution, spleen and LN cells were isolated and CD4$^+$ cells were stained intracellularly for Foxp3 in respective compartments. Representative plot showing Foxp3 staining in CD4$^+$ T cells 1B3.RAG or WT compartments (left) and graph showing pooled data (right) are shown with bar representing mean. Data are representative of two independent experiments.

Interestingly, multiple canonical T reg markers, including Foxp3, CD25, GITR, and CTLA-4, did not differ among the different T cell subsets (Fig. 2 a and not depicted).

Further analyses were performed on Nrp-1 as prior studies have shown reduced Nrp-1 on different iT reg cell populations generated in vivo (Feuerer et al., 2010). Nearly 70% of Foxp3$^+$ T reg cells expressed Nrp-1 in WT NOD or B6 mice correlating with Helios expression (Fig. 2 c; Thornton et al., 2010), suggesting that Nrp-1^{hi} T reg cells were thymically derived, whereas Nrp-1^{lo} T reg cells represented a peripherally derived T reg cell subset. To further confirm that Nrp-1^{lo}Foxp3$^+$ T reg cells in conventional mice resembled the iT reg cells seen in 1B3.RAG$^{-/-}$ mice, we examined selected mRNAs differentially expressed between 1B3 T reg cells and 1B3.RAG$^{-/-}$ iT reg cells in the microarray analyses. Several genes, including Eos, Tnfrsf9, and Lypd1, showed detectable mRNA levels in the T reg subsets by real time PCR. All of these transcripts showed elevated expression in Nrp-1^{hi} compared with Nrp-1^{lo} T reg cells (Fig. 2 d). Importantly, the Nrp-1^{hi} and Nrp-1^{lo} T reg cells expressed the same high levels of Foxp3. Although there were both Nrp-1^{hi}– and Nrp-1^{lo}–expressing CD4$^+$CD8$^-$Foxp3$^+$ T reg cells in the thymus, the overwhelming majority of the Nrp-1^{lo} cells were present within the immature CD24^{hi}Qa-2^{lo} subset, whereas the vast majority of the mature CD24^{lo}Qa-2hi^{hi} were Nrp-1$^+$ (Fig. 2 e and Fig. S3 a). Although these results cannot rule out that a rare Nrp-1^{lo} population might emigrate from the thymus, the bulk of the data in Figs. 1 and 2 are most consistent with Nrp-1 distinguishing thymically derived nT reg from the peripheral iT reg population.

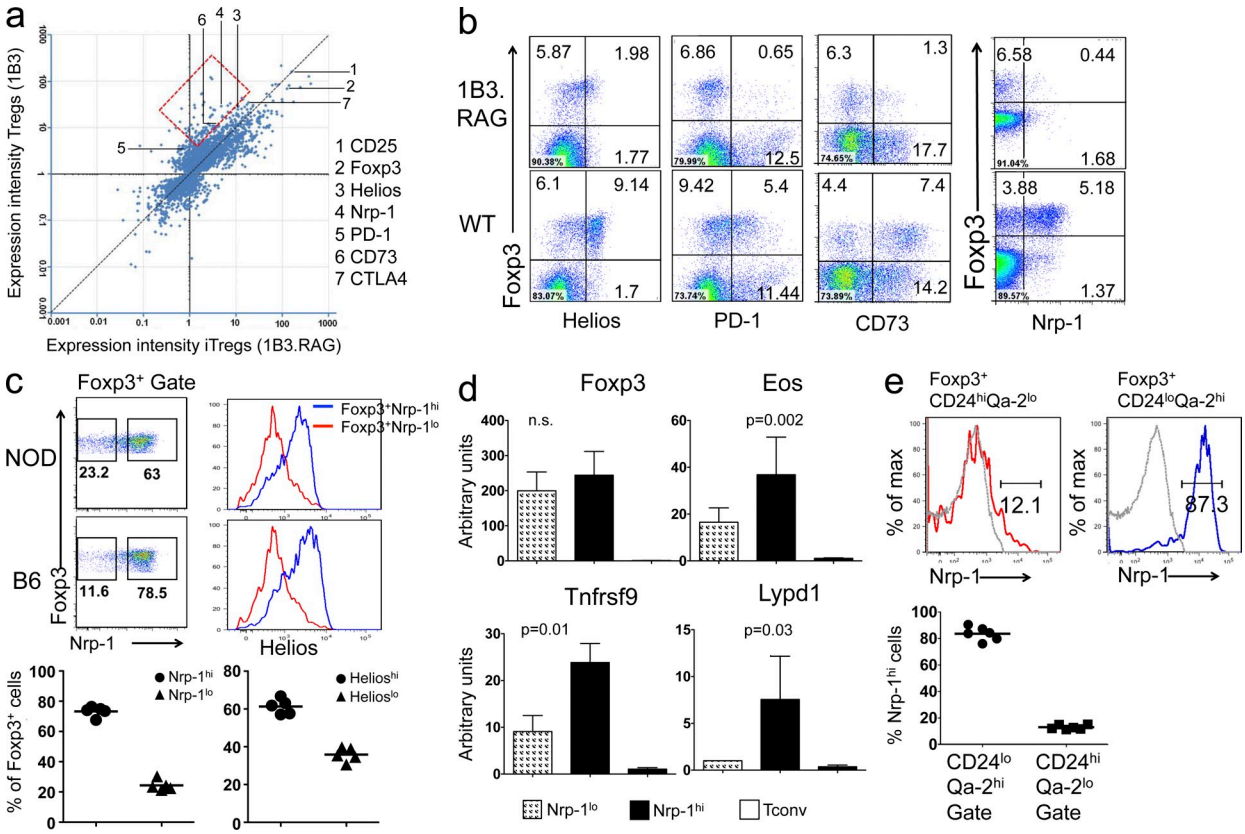

Figure 2. Nrp-1 is differentially expressed on natural and iT reg cells. (a) Expression plots showing the relative intensity of gene expression in iT reg cells (1B3.RAG$^{-/-}$) and nT reg cells (1B3). The y axis compares the expression profiles of T reg cells from 1B3 mice, whereas the x axis compares the expression profiles of iT reg cells from 1B3.RAG$^{-/-}$ mice (mean values are shown from $n = 4$ each group). Selected genes are marked and genes up-regulated specifically in nT reg cells are highlighted in the box. (b) CD4$^+$ T cells from LNs (pooled) of 1B3.RAG$^{-/-}$ or WT-NOD (4–5 wk) mice were stained with Nrp-1, PD-1, CD73, Foxp3, and Helios. (c) CD4$^+$ cells from LN (pooled) of NOD, or B6 WT mice were stained with Foxp3 and Nrp-1. Foxp3$^+$ T cells were gated into Nrp-1^{hi} and Nrp-1^{lo} subsets and analyzed for Helios expression (histograms). Graphs (bottom) compare percentages of Nrp-1– and Helios-positive cells among Foxp3$^+$ T reg cells from five individual mice (NOD) with bars representing means. (d) Relative mRNA expression levels of Foxp3, Eos, Tnfrsf9, and Lypd1 in Foxp3.GFP$^+$Nrp-1^{hi} (Nrp-1^{hi}) or Foxp3.GFP$^+$Nrp-1^{lo} (Nrp-1^{lo}) or CD4$^+$Foxp3.GFP$^-$ (T conv) cells (mean ± SD from four replicates). (e) Foxp3$^+$ cells in CD4 single-positive thymocytes of a 5-wk-old NOD mouse were separated into CD24^{hi}Qa-2^{lo} and CD24^{lo}Qa-2^{hi} and analyzed for Nrp-1 staining (representative histogram is shown; dotted line is isotype control). Percentages of Nrp-1^{hi} cells in both Foxp3$^+$ subsets are shown with each dot representing an individual mouse and bars representing means.

iT reg cells generated in vitro or in vivo lack Nrp-1 expression

Stimulation of CD4$^+$CD25$^-$ conventional T (T conv) cells with either antigen-loaded APCs or anti-CD3 plus anti-CD28 beads in the presence of TGF-β results in the induction of Foxp3$^+$ T reg cells (Chen et al., 2003). Despite expressing high levels of Foxp3, in vitro generated T reg cells expressed little or no Nrp-1 (Fig. 3 a). Several models of antigen-induced conversion of T conv cells into iT reg cells in vivo have been developed by altering antigen dose or route of antigen administration (Apostolou and von Boehmer, 2004). First, we examined Nrp-1 expression on iT reg cells generated in vivo through the homoeostatic conversion of naive T cells. Naive CD4$^+$ T cells were transferred into RAG-deficient mice and monitored for Nrp-1 expression as they converted into T reg cells. Foxp3$^+$ T reg cells induced 2 wk after transfer exhibited an Nrp-1^{lo} phenotype (Fig. 3 b).

Next, we examined the expression of Nrp-1 in the setting of prolonged low-dose antigen administration (Apostolou and von Boehmer, 2004) by exposing T reg–deficient, OVA-specific TCR Tg (DO11) RAG$^{-/-}$ mice to a subimmunogenic regimen of OVA peptide (0.1 or 1 μg per day) over a 2-wk time period. As shown in Fig. 3 c, T reg cells from DO11.RAG$^{+/+}$ exhibited both Nrp-1^{hi}– and Nrp-1^{lo}– expressing T reg cells, whereas iT reg cells generated in OVA-treated DO11.RAG$^{-/-}$ mice were predominantly Nrp-1^{lo}. These results confirmed our findings from 1B3.RAG$^{-/-}$ mouse that iT reg cells are largely deficient in Nrp-1 expression. Finally, we examined Nrp-1 expression on resident T reg cells in the gut-associated lymphoid tissue, which is a preferential site for the peripheral induction of Foxp3$^+$ T reg cells. As shown in Fig. 3 d, analysis of CD4$^+$ T cells from the colonic lamina propria revealed that a majority of Foxp3$^+$ T reg cells in this tissue expressed low levels of Nrp-1, a phenotype distinct

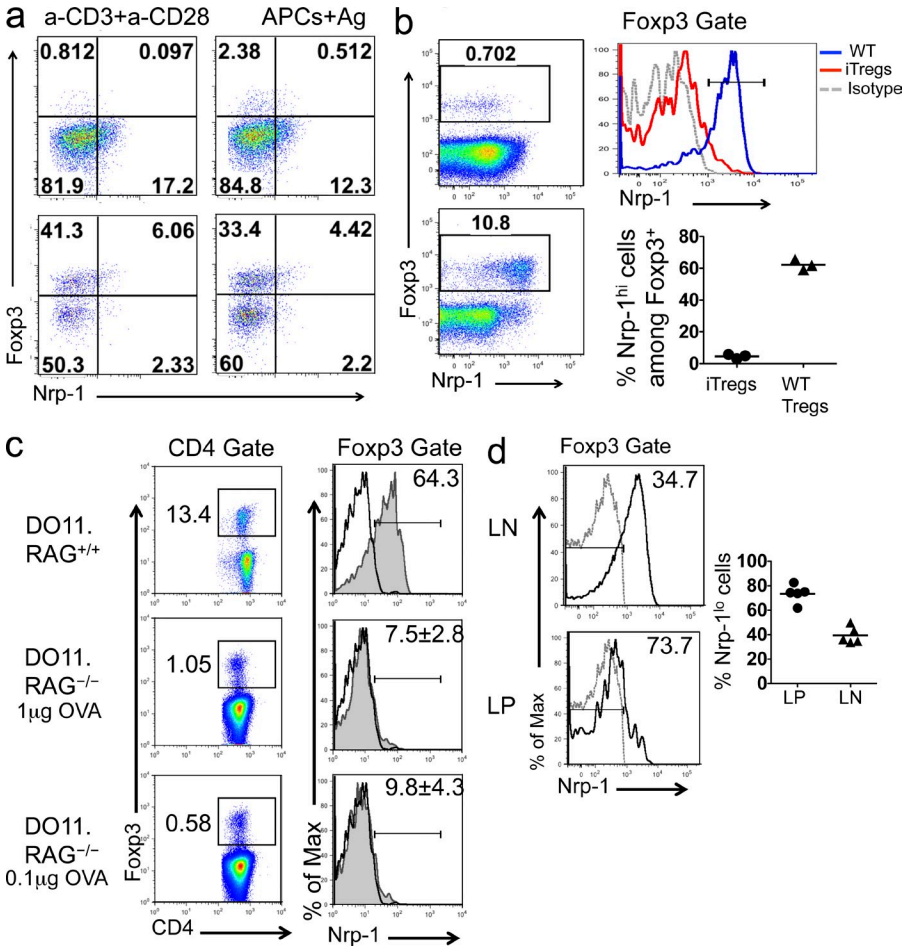

Figure 3. Peripherally generated Foxp3⁺ iT reg cells lack Nrp-1 expression. (a) Cells from 1B3.Foxp3-GFP mice were sorted into T conv ($CD4^+CD25^-Foxp3^-$) cells and stimulated in vitro with anti-CD28 plus anti-CD28 Abs or with irradiated spleen cells loaded with 1B3 cognate peptide in the absence (top) or presence (bottom) of TGF-β. After 5 d of incubation, live $CD4^+$ cells were stained for Nrp-1 and Foxp3. One representative plot from triplicate wells is shown and is representative of three independent experiments. (b) Naive T cells ($CD4^+CD25^-GITR^-CD62L^+$) were transferred into $RAG^{-/-}$ recipient mice. 2 wk after transfer, $CD4^+$ T cells from LN were stained with Foxp3 and analyzed for Nrp-1 expression. Histogram overlay showing Nrp-1 expression on converted iT reg cells compared with T reg cells in LN of WT mouse is shown. Bottom right, graph shows Nrp-1 expression on iT reg cells or WT in LN from three individual mice and bar represents mean. Data are representative of two independent experiments. (c) Foxp3 staining in $CD4^+$ from inguinal LN of DO11.$RAG^{-/-}$ mice 2 wk after implantation of osmotic pumps delivering PBS or 0.1 μg or 1 μg of OVA peptide per day ($n = 3$ for each group). Representative plots showing Nrp-1 staining (filled histogram) or isotype control Ab (empty histograms) on gated $Foxp3^+$ cells is shown with numbers depicting mean ± SD of $Nrp\text{-}1^{hi}$ cells from three different mice. LN from untreated DO11.$RAG^{+/+}$ mice was used as a control. (d) Foxp3 staining in $CD4^+$ cells from axillary LN (LN) or lamina propria of colon (LP) from 8–12-wk-old NOD mouse. Representative histograms showing Nrp-1 staining (solid) or isotype control Ab (dotted line) on gated $Foxp3^+$ cells are shown. Numbers indicate percentage of $Nrp\text{-}1^{lo}$ cells in the gate. Graph with percentage of $Nrp\text{-}1^{lo}$ among $Foxp3^+$ cells from five mice is shown on right, with bars representing means.

from LN T reg cells (Fig. 3 d and Fig. S3 b). Together, the in vitro and in vivo data, combined with the resident gut T reg cell data, strongly support the conclusion that Nrp-1 distinguishes thymically derived nT reg cells from iT reg cells. We suggest that Nrp-1 may be a more reliable marker than Helios under certain conditions, as we and others (Akimova et al., 2011; Gottschalk et al., 2012) have seen that iT reg cells up-regulate Helios expression in some settings (not depicted). Moreover, unlike Helios, Nrp-1 is a cell surface molecule that can be efficiently used to separate inducible versus nT reg cell subsets under homeostatic conditions.

Nrp-1 expression on T reg cells is not significantly altered by activation

Next, we tested whether differential Nrp-1 expression on T reg cells was a consequence of activation status of the cells. T reg cells from 1B3 mice were sorted into $Nrp\text{-}1^{hi}$ and $Nrp\text{-}1^{lo}$ T reg cells and activated with APCs loaded with 1B3 cognate peptide for 72 h. As shown in Fig. 4 a, both $Nrp\text{-}1^{hi}$ and $Nrp\text{-}1^{lo}$ cells maintained Nrp-1 expression (either high or low, respectively) on both $CD69^+$ and $CD69^-$ subsets. Interestingly, Nrp-1 was up-regulated on some activated T conv cells suggesting a transient expression, unlike nT reg cells where it is stably expressed. Similar results were observed with NOD T reg cells using anti-CD3 and anti-CD28 mAb activation (unpublished data).

To test stability of Nrp-1 expression in vivo, $Nrp\text{-}1^{hi}$ or $Nrp\text{-}1^{lo}$ T reg cells from NOD.Thy1.1 mice were sorted and transferred into Thy1.2 recipients. Under these homeostatic conditions, both the T reg subsets exhibited a stable phenotype and maintained equivalent levels of Foxp3. Most importantly, levels of Nrp-1 expression, high versus low, remained stable and similar to the levels of the injected cell subsets (Fig. 4 b). A similar trend was seen when $Nrp\text{-}1^{hi}$ or $Nrp\text{-}1^{lo}$ T reg cells were transferred into lymphopenic hosts although Nrp-1 expression was up-regulated on some $Nrp\text{-}1^{lo}$ T reg cells under these conditions (Fig. 4 c). These results suggest that low Nrp-1 expression may not be an immutable feature of iT reg cells and could be up-regulated on a subset of cells in certain proinflammatory environments. Further studies will

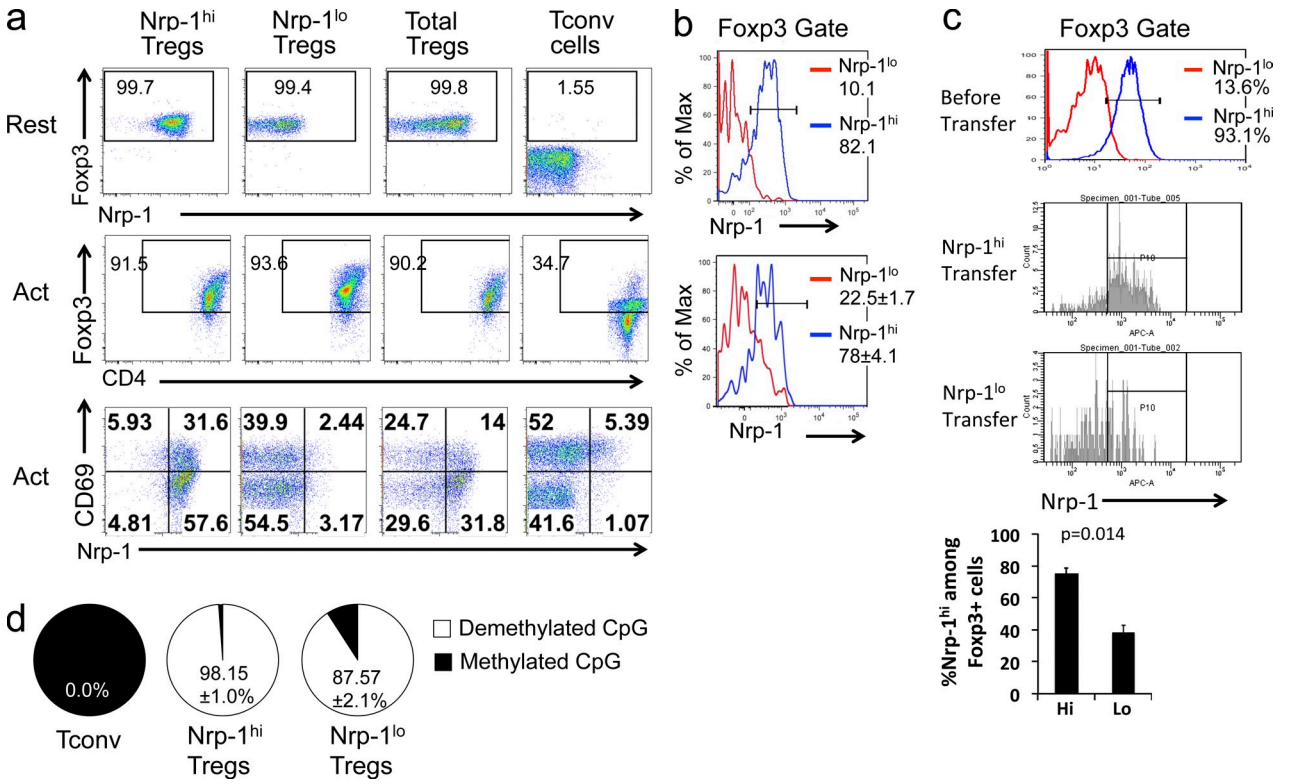

Figure 4. Nrp-1 expression is not significantly altered by activation. (a) Cells from 1B3.Foxp3-GFP mice were sorted into T conv ($CD4^+Foxp3^-$) or T reg cells (separated into $Nrp\text{-}1^{lo}$, $Nrp\text{-}1^{hi}$, or total) and activated in vitro with irradiated spleen cells loaded with 1B3 cognate peptide for 72 h. Resting state cells are shown on the top. After activation, CD4 cells were stained with Foxp3 (middle) or with CD69 and Nrp-1 (bottom). Live cells gated on $CD4^+$ are shown from one of three replicates. Data are representative of three independent experiments. (b) 2.5×10^5 T reg cells ($Nrp\text{-}1^{hi}$ or $Nrp\text{-}1^{lo}$) from NOD.Thy1.1 mice were adoptively transferred into a WT Thy1.2 congenic host. Histograms show relative Nrp-1 expression in $Nrp\text{-}1^{hi}$ or $Nrp\text{-}l^{lo}$ T reg cells before (top) and 1 wk after transfer (bottom). Numbers in the bottom depict mean ± SD of Nrp^{hi} cells (among $Foxp3^+$) from three different mice. Data are representative of two independent experiments. (c) 1.5×10^5 $Foxp3^+Nrp\text{-}1^{hi}$ or $Foxp3^+Nrp\text{-}1^{lo}$ T reg cells were sorted from a $WT.Thy1.1^+$ mouse and transferred into RAGKO mice with similar number of congenically marked T conv ($CD4^+Foxp3^-$) cells. 1 wk after transfer, $Thy1.1^+CD4^+Foxp3^+$ T cells from spleen and LN were analyzed for Nrp-1 expression. Top histograms show Nrp-1 staining before transfer, and a representative plot with Nrp-1 expression after transfers with $Nrp\text{-}1^{hi}$ or $Nrp\text{-}1^{lo}$ T reg cells is shown. Bottom graph depicts mean + SD with data from four mice showing Nrp-1 staining on $Foxp3^+$ cells in T reg compartment (Thy1.1). Data are representative of two independent experiments. (d) Methylation status of CpG motifs of the TSDR of the Foxp3 locus in different T reg cell subsets. $Foxp3^+Nrp\text{-}1^{hi}$ or $Foxp3^+Nrp\text{-}1^{lo}$ T reg cells or $Foxp3^-$ T conv cells were isolated from NOD.Foxp3-GFP mouse. Numbers in the pie chart indicate mean ± SD of percent demethylation in the population from six replicates.

be required to determine if specific conditions can up-regulate Nrp-1 expression on iT reg cells.

Epigenetic modulation in the Foxp3 locus leading to demethylation of CpG islands in the region of Foxp3 locus (TSDR) is a hallmark of nT reg cells and is thought to reflect stable, constitutive Foxp3 expression in this population. Bisulfite sequence analysis confirmed that 100% of $CD4^+Foxp3.GFP^-$ T conv cells had methylated CpG sites, whereas >98% of CpG sites were demethylated in $Nrp\text{-}1^{hi}$ nT reg cells (Fig. 4 d). Notably, $Nrp\text{-}1^{lo}$ iT reg cells also displayed a highly demethylated TSDR but had slightly but significantly lower demethylation than $Nrp\text{-}1^{hi}$ T reg cells (87.5 compared with 98% , $P < 0.001$). This might reflect the newly generated $Foxp3^+$ cells among $Nrp\text{-}1^{lo}$ T reg cells, which have not yet fully stabilized the Foxp3 expression. In vivo generated iT reg cells previously have been shown to exhibit demethylated TSDR (Polansky et al., 2008) and methylated TSDR (Haribhai et al., 2011), which highlights differences in the models used and the heterogeneity of this population. By comparison, a study by Miyao et al. (2012) showed that iT reg cells once stabilized in vivo display demethylated TSDR.

iT reg cells can suppress ongoing autoimmune response

Despite the presence of $Foxp3^+$ iT reg cells in the periphery of $1B3.RAG^{-/-}$ mice, the animals developed EAE by 3–4 wk of age. These results suggested that the peripherally generated T reg cells could not control autoimmunity in this setting. However, iT reg cells from $1B3.RAG^{-/-}$ exhibited excellent suppressive ability and inhibited proliferation of 1B3 T conv cells (responder T [T resp] cells) equally or better than nT reg cells (from 1B3 mice) at various ratios of T resp/T reg cells tested in vitro (Fig. 5 a). We speculate that iT reg cells in $1B3.RAG^{-/-}$ mice were being generated in inflammatory and lymphopenic environment, which could

compromise their activity. Consistent with this hypothesis, we observed that Nrp-1^{lo} T reg cells from the 1B3 mouse were less effective in controlling EAE when transferred together with naive T cells into RAG$^{-/-}$ mice when compared with Nrp-1^{hi} cells. Not only did Nrp-1^{lo} T reg cells fail to control EAE, the cells down-regulated Foxp3 expression in this lymphopenic setting (Fig. 5, b and c).

However, the Nrp-1^{lo} T reg cells were able to suppress autoimmunity in both a lymphodeficient and a lymphosufficient autoimmune setting when using another TCR Tg mouse, the chromogranin A–specific BDC2.5 model. Previous studies have shown spontaneous diabetes could be prevented by injection of islet antigen-specific BDC2.5 TCR Tg T reg cells into NOD.CD28$^{-/-}$ or BDC2.5 T effector cell reconstituted NOD.RAG$^{-/-}$ mice before the disease onset (Tang et al., 2004). Therefore, we transferred Nrp-1^{hi} or Nrp-1^{lo} BDC2.5 T reg cells into prediabetic NOD.CD28$^{-/-}$ mice and monitored diabetes. Both Nrp-1^{hi} and Nrp-1^{lo} BDC2.5 T reg cells were equally effective in preventing the development of diabetes in CD28$^{-/-}$ mice (Fig. 5 d). Similar preliminary results have been observed in the RAG-deficient adoptive transfer setting (not depicted). Different results in the alternative model systems (1B3 vs. BDC2.5) may reflect differences in TCR affinity or specificity, which may affect T reg cell function or stability. This concept is supported by the reduced stability of the iT reg population seen in this environment (Fig. 5 c; Duarte et al., 2009). Hence, careful analyses will determine whether iT reg cells with distinct TCR specificity function differently in various immune settings. This will be crucial in understanding whether iT reg cells merely complement nT reg cells or play a larger role in maintaining tolerance, especially given data suggesting that blocking of Nrp-1 abrogates suppression of proliferation of responder T cells by T reg cells (Sarris et al., 2008).

In summary, the extensive studies described in this paper demonstrate that the cell surface marker Nrp-1 distinguishes nT reg from iT reg cells generated in several different immune settings including low-dose antigen-induced iT reg cells, T reg cells in intestinal lamina propria, iT reg cells generated spontaneously in 1B3.RAG$^{-/-}$ mice or through conversion in vivo, and T reg cells generated in vitro using TGF-β. Moreover, our thymus data showing that mature Foxp3^{+} T reg cells express the highest levels of Nrp-1 strongly suggest that the overwhelming majority of thymically derived T reg cells express Nrp-1. Although it remains possible that a small subset of Nrp-1^{lo} T reg cells leave the thymus, T reg cells generated in the periphery are uniformly Nrp-1^{lo}, whereas Nrp-1^{hi} T reg cells are always thymically derived. This ability to separate different subtypes of T reg cells will be useful in studying their role and contribution in autoimmune disease. Finally, although human T reg cells in peripheral blood do not express

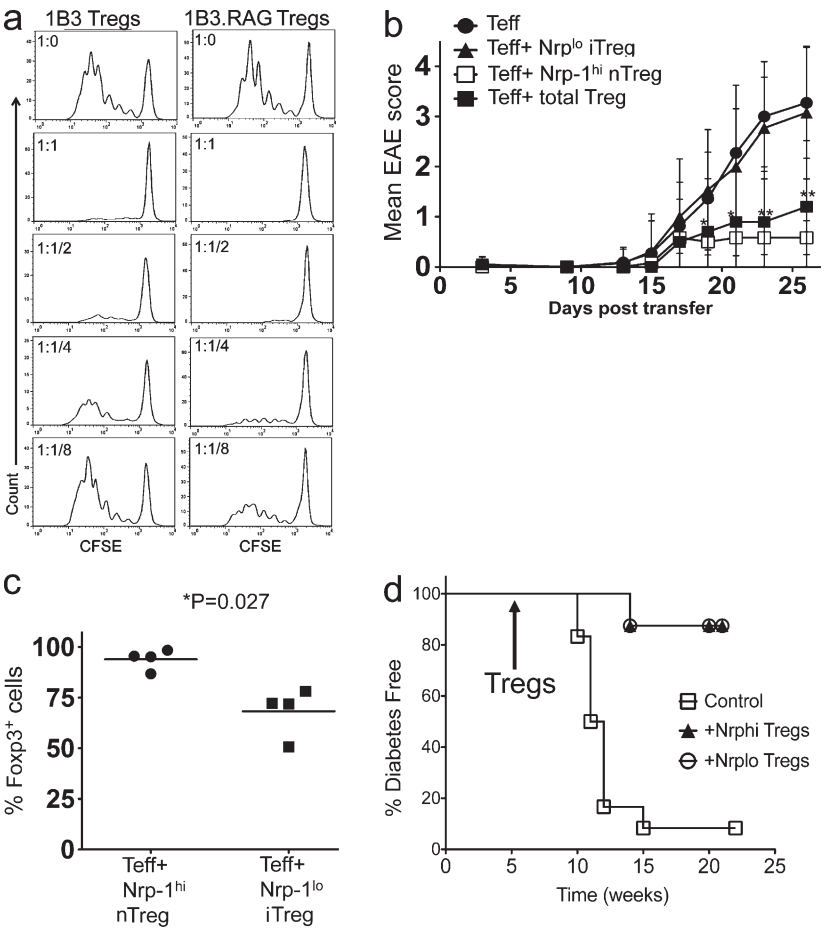

Figure 5. Suppressive activity of Nrp-1^{lo} iT reg cells in vitro and in vivo. (a) CFSE-labeled CD4^{+} T conv cells from 1B3.Thy1.1 mice were cultured in the presence of irradiated APCs and 1B3 peptide with or without different ratios of T reg cells from 1B3. RAG-sufficient or 1B3.RAG$^{-/-}$ mice. 3 d later, cells were analyzed for CFSE dilution by flow cytometry. (b) T reg cells were sorted based on CD4, CD25, and GITR expression to select total T reg cells followed by an additional separation based on Nrp-1^{hi} (nT reg cells) and Nrp-1^{lo} (iT reg cells). 5 × 10^{4} 1B3.Thy1.2 CD4^{+}CD25^{-} T conv cells (Teff) were co-transferred with or without similar number of Nrp-1^{hi} or Nrp-1^{lo} or total T reg cells from 1B3.Thy1.1 mice in the RAG$^{-/-}$ recipients and monitored for EAE development. The data are presented as the mean EAE score, with error bars showing SD, and are representative of four independent experiments. n = 12 for Teff+nT reg; n = 13 for Teff+iT reg; n = 11 for Teff; and n = 10 for Teff+Total T reg cells. *, P < 0.05; **, P < 0.001 for Teff+nT reg versus Teff+iT reg. (c) Foxp3 staining in the T reg compartment in different transfer groups at the end of the disease (bars show means). (d) Prediabetic NOD.CD28$^{-/-}$ mice were injected with 5 × 10^{4} Nrp-1^{hi} nT reg (n = 8) or Nrp-1^{lo} iT reg cells (n = 8) from BDC.2.5-TCR-Tg mice or left untreated (n = 12 each). The development of diabetes was monitored by measuring blood glucose of individual mice. Mice with two consecutive readings of blood glucose >250 mg/dl were labeled diabetic.

Nrp-1, T reg cells in secondary lymphoid organs have been shown to express Nrp-1 (Battaglia et al., 2008; Milpied et al., 2009). A similar separation of T reg cells into natural and iT reg subsets in human would be useful in the study of human T reg cells and their use in clinical cell-based therapies.

MATERIALS AND METHODS

Mice. NOD.POT (P0-specific TCR-Tg mouse), NOD.Foxp3-GFP-Cre reporter mice have been previously described (Louvet et al., 2009; Zhou et al., 2009). C57BL/6, NOD, NOD-B7-2$^{-/-}$, NOD-TCR$\alpha^{-/-}$, and NOD-RAG2$^{-/-}$ mice were bred in our facility. All mice were housed in a specific pathogen-free University of California, San Francisco (UCSF) facility. The Institutional Animal Care and Use Committee of UCSF approved all animal experiments.

Flow cytometry. For analysis of surface markers, cells were stained in FACS buffer (PBS containing 2% wt/vol BSA) and the appropriate antibodies. Unless stated, all antibodies for cell surface markers and the anti-Helios mAb were purchased from BioLegend. Anti–Nrp-1 Ab was purchased from R&D Systems. Anti–PD-1 mAb and anti-Foxp3 mAb was purchased from eBioscience. Foxp3 staining was done according to the manufacturer's instructions (eBioscience). For cytokine analysis, cells were incubated for 3–4 h at 37°C with 0.5 M ionomycin, 10 ng/ml of PMA, and 3 M monensin before being fixed and made permeable (Foxp3 Staining kit; eBioscience) and were stained for intracellular proteins. Stained cells were analyzed with FACSCalibur or an LSR II (BD) and data were analyzed using FlowJo software (Tree Star). T cells were sorted with a MoFlo high-speed cell sorter (Dako) or FACSAria (BD).

Generation of 1B3 TCR-Tg mice. Cells from sciatic nerves of neuropathic NOD-B7-2$^{-/-}$ mice were prepared as previously described (Louvet et al., 2009). In brief, CD4$^+$CD8$^-$ cells were sorted and expanded with anti-CD3– and anti-CD28–coated beads supplemented with 2,000 IU/ml rhIL-2, as previously described (Tang et al., 2004). The expanded CD4$^+$ T cells were fused to the TCR-negative thymoma partner BW1100 (provided by E. Palmer, University Hospital Basel, Basel, Switzerland) using standard protocols. TCR-expressing hybridoma clones were tested for antigen specificity by incubating 50,000 cells with 0.2×10^6 APCs (NOD-TCR-αKO spleen cells, irradiated NOD spleen cells, or NOD BM-derived DCs) with different nerve lysates for 16–24 h, followed by staining with CD69. From the 1B3 hybridoma cDNA, the full-length coding sequences for the TCR-α and -β chains were cloned by PCR and were subcloned into a CD2 and CD4 expression vector, respectively, allowing expression of the transgenes in both CD4 and CD8 T cells (Wang et al., 2001). Tg mice were generated by microinjection of CD2–TCR-α and CD4–TCR-β constructs into NOD embryos as described earlier (Louvet et al., 2009). Vectors were provided by N. Killeen (UCSF, San Francisco, CA). Overlapping MBP peptides spanning the sequence of mouse MBP were synthesized by Genemed or were synthesized by J. Wouter and C.J.M. Melief (Leiden University, Leiden, Netherlands).

Gene array. Sorted T reg cells (CD4$^+$CD25$^+$GITR^{hi} with >95% purity) from WT, 1B3, or 1B3.RAG$^{-/-}$ mice were used for isolation of Total RNA. Total RNA from each paw was amplified for one round using the Message Amp II amplified RNA (aRNA) Amplification kit (Ambion), labeled using a modified protocol with the ULS aRNA Fluorescent Cy5 labeling kit (Kreatech Diagnostics), and purified using RNA Clean and Concentrate spin columns according to manufacturer's protocol (Zymo Research Corporation). aRNA was hybridized to 4 × 44K Mouse Whole Genome Microarrays (Agilent Technologies) for 18 h according to the manufacturer's protocol. Microarrays were washed in 0.01× SSC/0.005% Triton X-102 at 40°C, dried with HEPA filtered compressed nitrogen and scanned on a DNA Microarray Scanner (Agilent Technologies) at a 5-µm resolution. Data were extracted from the scanned image using Feature Extraction Software (Agilent Technologies) and were further processed for background subtracted and signal normalization.

Thymectomy and intrathymic injections. The thymus was removed from 2–3- or 10–14-d-old mice by suction under anesthesia. The wound was glued and the mice were kept at 30°C overnight and then returned to their mothers. Thymectomy was confirmed by visual examination at autopsy and only mice with complete thymectomy were included in the experiments. For intrathymic injections mice were anesthetized with acepromazine, ketamine, and xylazine, the sternum was cut open to access the thymus. 1×10^7 total thymocytes were injected in 10-µl suspension into the thymus of 4–6-wk-old WT NOD.Thy1.1 mice. Animals were placed on a heat pad until they regained consciousness. After 4 d, mice were sacrificed and single cell suspensions were prepared from whole thymuses and stained for surface markers and intracellularly for Foxp3 and analyzed by flow cytometry.

Mixed bone marrow chimera. 1B3.RAG$^{-/-}$ or NOD bone marrow was mixed with NOD.Thy1.1 bone marrow at a ratio of 1:1 (1×10^6) and co-injected into sublethally irradiated RAG$^{-/-}$ recipients (400 rads) to generated mixed chimera. After 6 wk, the thymus, peripheral LN and spleen were analyzed by flow cytometry for expression of Nrp-1, PD-1, Helios, and Foxp3 on CD4$^+$ T cells in Thy1.1 or Thy1.2$^+$ fractions.

T reg cells in prevention of diabetes in vivo in NOD.CD28$^{-/-}$ mice. Nrp-1^{hi} or Nrp-1^{lo} T reg cells were sorted from NOD.BDC2.5.Foxp3-GFP mouse. 5×10^4 sorted T reg cells were adoptively transferred in 5–6-wk-old prediabetic male NOD.CD28$^{-/-}$ mice. Nonfasting blood glucose levels in recipient mice were monitored every week using a One-touch Ultra glucometer (Lifescan Inc.). Mice with two consecutive blood glucose readings over 250 mg/dl were considered diabetic.

Foxp3$^+$ iT reg cell in vitro activation. For in vitro activation, T cells from 1B3.Foxp3-GFP mice were sorted into T conv (CD4$^+$Foxp3$^-$) or T reg cells (separated into Nrp-1^{lo}, Nrp-1^{hi}, and total) and activated in vitro with irradiated splenocytes loaded with 1B3 peptide (SRPGLCHMYKDS) or with anti-CD3 and anti-CD28 beads for 72 h. At the end of incubation, cells were stained with CD4 and Foxp3 or with CD69 and Nrp-1.

Foxp3$^+$ iT reg cell conversion. Freshly sorted T conv cells (CD4$^+$CD25$^-$Foxp3$^-$) from spleen and LN of 1B3.Foxp3-GFP mouse were cultured for 5 d with anti-CD3 and anti-CD28 microbeads or irradiated splenic cells loaded with 1B3 cognate (SRPGLCHMYKDS) peptide and IL-2 in the presence or absence of TFG-β. After incubation T cells were then collected and live cells were stained for intracellular Foxp3 and surface markers. For in vivo conversion, 10^6 naive T cells (CD4$^+$CD25$^-$CD62L$^+$GITR$^-$) were adoptively transferred into RAG$^{-/-}$ mice. 2 wk later, CD4$^+$ T cells from spleen and LN were stained for Foxp3 and Nrp-1.

Induction of iT reg cells in DO11.RAG$^{-/-}$ mice. Osmotic pump (ALZET1002; Durect Corporation) infusing either 0.1 µg or 1 µg OVA peptide (323–339) or PBS per day was implanted s.c. in DO11.RAG$^{-/-}$ mice as described previously (Apostolou and von Boehmer, 2004). After 14 d, inguinal LN and spleen were harvested and CD4$^+$ cells were surface stained for Nrp-1 and intracellularly for Foxp3. 3 DO11.RAG$^{-/-}$ mice per group were used and unimmunized DO11.RAG$^{+/+}$ was used as control.

Isolation of lamina propria cells. Colons were harvested from 8–10-wk-old NOD mice sliced and digested by 0.07 U/ml Liberase Blendzyme III and 0.5 mg/ml DNase 1. LN cells were also subjected to similar treatment. The cells were resuspended in 40% Percoll and carefully overlaid onto 70% Percoll. The interface containing the lamina propria leukocytes was collected. Harvested cells were surface stained for CD4, Nrp-1, and intracellularly for Foxp3.

TSDR methylation assay. A quantitative real-time PCR method was developed to analyze the methylation status of key CpG dinucleotides in the TSDR of the FOXP3 gene where demethylation has been shown to correlate with stable T reg cells (Floess et al., 2007). T conv, Nrp-1^{lo}, and Nrp-1^{hi} (2×10^5 each) were sorted from Foxp3.GFP mouse and processed using the EZ DNA Methylation-Direct kit (Zymo Research) according to the manufacturer's protocol. Purified bisulfite-treated DNA was used in a quantitative PCR reaction. Primers and probes were designed using Primer Express software (Applied Biosystems) with TSDR DNA sequence that had been bisulfite converted in silico using Methyl primer Express software (Applied Biosystems). Sequences used were the following: forward primer, 5′-GGTTTATATTTGGGTTTTGTTGTTA-TAATTT-3′; and reverse primer, 5′-CCCCTTCTCTTCCTCCTTAT-TACC-3′. Probe sequences were: methylated (CG) probe, 5′-TGACGT-TATGGCGGTCG-3′; and unmethylated (TG) probe, 5′-ATTGATGT-TATGGTGGTTGGA-3′. PCR was performed with 10 µl Universal Master Mix II (Applied Biosystems), 1 µl eluted DNA, primer/probe mix, and enough water to bring total volume to 20 µl. Final concentration of primers was 900 nM and concentration of probes was 150 nM. Reactions were run for 10 min at 95°C for 10 min and 50 cycles of 95°C for 15 s and 61°C for 1.5 min (7500 Real-Time PCR System; Applied Biosystems). Percent demethylation was calculated using the formula percent demethylation = $100/[1 + 2^{(CtTG - CtCG)}]$, where CtTG represents the threshold cycle of the TG (unmethylated) probe and CtCG represents the threshold cycle of the CG (methylated) probe (Cottrell et al., 2007).

Statistical analysis. Statistical analysis was done using Prism software (GraphPad Software). Statistical analysis was performed using a two-tailed Student's *t* test.

Online supplemental material. Fig. S1 depicts the generation and characterization of 1B3 TCR Tg mouse. Fig. S2 shows the heat map of selected genes that were differentially regulated between 1B3.RAG$^{-/-}$ and NOD and 1B3 T reg cells. Fig. S3 shows the gating strategy for Fig. 2 e and Fig. 3 d. Table S1 shows the full list of genes differentially regulated between 1B3.RAG$^{-/-}$ and NOD and 1B3 T reg cells with a fold discovery rate of ≤0.01. Online supplemental material is available at http://www.jem.org/cgi/content/full/jem.20120822/DC1.

We thank M. Lee, N. Grewal, and S. Jiang, for technical assistance; J. J. Lozano for helping with microarray analysis; D. Fuentes for animal husbandry; and A. Abbas, Q. Tang, H. Bour-Jordan, M. Anderson, and members of the Bluestone laboratory for discussions.

This work was supported by the US National Institutes of Health (R01 AI50834 and P30DK63720) and a grant from Pfizer.

The authors declare no competing financial interests.

M. Yadav designed and did experiments, analyzed data, and wrote the manuscript; C. Louvet designed and did experiments; J.M. Gardner and D. Davini did experiments; R. Head and D. Weiss did Microarray design, data generation, analysis, and interpretation; M. Martinez-Llordella, D.J. Kuster, and D. Von Schack did microarray analysis and interpretation; S. Bailey-Bucktrout helped with data analysis; F.M. Sverdrup and B.A. Anthony performed the TSDR analyses; and J.A. Bluestone designed experiments, supervised the work, analyzed data, and wrote the manuscript.

Submitted: 16 April 2012
Accepted: 14 August 2012

REFERENCES

Akimova, T., U.H. Beier, L. Wang, M.H. Levine, and W.W. Hancock. 2011. Helios expression is a marker of T cell activation and proliferation. *PLoS ONE*. 6:e24226. http://dx.doi.org/10.1371/journal.pone.0024226

Apostolou, I., and H. von Boehmer. 2004. In vivo instruction of suppressor commitment in naive T cells. *J. Exp. Med*. 199:1401–1408. http://dx.doi.org/10.1084/jem.20040249

Battaglia, A., A. Buzzonetti, G. Monego, L. Peri, G. Ferrandina, F. Fanfani, G. Scambia, and A. Fattorossi. 2008. Neuropilin-1 expression identifies a subset of regulatory T cells in human lymph nodes that is modulated by preoperative chemoradiation therapy in cervical cancer. *Immunology*. 123:129–138. http://dx.doi.org/10.1111/j.1365-2567.2007.02737.x

Bautista, J.L., C.W. Lio, S.K. Lathrop, K. Forbush, Y. Liang, J. Luo, A.Y. Rudensky, and C.S. Hsieh. 2009. Intraclonal competition limits the fate determination of regulatory T cells in the thymus. *Nat. Immunol*. 10:610–617. http://dx.doi.org/10.1038/ni.1739

Bennett, C.L., J. Christie, F. Ramsdell, M.E. Brunkow, P.J. Ferguson, L. Whitesell, T.E. Kelly, F.T. Saulsbury, P.F. Chance, and H.D. Ochs. 2001. The immune dysregulation, polyendocrinopathy, enteropathy, X-linked syndrome (IPEX) is caused by mutations of FOXP3. *Nat. Genet*. 27:20–21. http://dx.doi.org/10.1038/83713

Bluestone, J.A., and A.K. Abbas. 2003. Natural versus adaptive regulatory T cells. *Nat. Rev. Immunol*. 3:253–257. http://dx.doi.org/10.1038/nri1032

Chen, W., W. Jin, N. Hardegen, K.J. Lei, L. Li, N. Marinos, G. McGrady, and S.M. Wahl. 2003. Conversion of peripheral CD4$^+$CD25$^-$ naive T cells to CD4$^+$CD25$^+$ regulatory T cells by TGF-β induction of transcription factor Foxp3. *J. Exp. Med*. 198:1875–1886. http://dx.doi.org/10.1084/jem.20030152

Cottrell, S., K. Jung, G. Kristiansen, E. Eltze, A. Semjonow, M. Ittmann, A. Hartmann, T. Stamey, C. Haefliger, and G. Weiss. 2007. Discovery and validation of 3 novel DNA methylation markers of prostate cancer prognosis. *J. Urol*. 177:1753–1758. http://dx.doi.org/10.1016/j.juro.2007.01.010

Duarte, J.H., S. Zelenay, M.L. Bergman, A.C. Martins, and J. Demengeot. 2009. Natural T reg cells spontaneously differentiate into pathogenic helper cells in lymphopenic conditions. *Eur. J. Immunol*. 39:948–955. http://dx.doi.org/10.1002/eji.200839196

Feuerer, M., J.A. Hill, K. Kretschmer, H. von Boehmer, D. Mathis, and C. Benoist. 2010. Genomic definition of multiple ex vivo regulatory T cell subphenotypes. *Proc. Natl. Acad. Sci. USA*. 107:5919–5924. http://dx.doi.org/10.1073/pnas.1002006107

Floess, S., J. Freyer, C. Siewert, U. Baron, S. Olek, J. Polansky, K. Schlawe, H.D. Chang, T. Bopp, E. Schmitt, et al. 2007. Epigenetic control of the foxp3 locus in regulatory T cells. *PLoS Biol*. 5:e38. http://dx.doi.org/10.1371/journal.pbio.0050038

Fousteri, G., J. Jasinski, A. Dave, M. Nakayama, P. Pagni, F. Lambolez, T. Juntti, G. Sarikonda, Y. Cheng, M. Croft, et al. 2012. Following the fate of one insulin-reactive CD4 T cell: conversion into Teffs and T regs in the periphery controls diabetes in NOD mice. *Diabetes*. 61:1169–1179. http://dx.doi.org/10.2337/db11-0671

Gottschalk, R.A., E. Corse, and J.P. Allison. 2012. Expression of Helios in peripherally induced Foxp3+ regulatory T cells. *J. Immunol*. 188:976–980. http://dx.doi.org/10.4049/jimmunol.1102964

Haribhai, D., J.B. Williams, S. Jia, D. Nickerson, E.G. Schmitt, B. Edwards, J. Ziegelbauer, M. Yassai, S.H. Li, L.M. Relland, et al. 2011. A requisite role for induced regulatory T cells in tolerance based on expanding antigen receptor diversity. *Immunity*. 35:109–122. http://dx.doi.org/10.1016/j.immuni.2011.03.029

Hill, J.A., M. Feuerer, K. Tash, S. Haxhinasto, J. Perez, R. Melamed, D. Mathis, and C. Benoist. 2007. Foxp3 transcription-factor-dependent and -independent regulation of the regulatory T cell transcriptional signature. *Immunity*. 27:786–800. http://dx.doi.org/10.1016/j.immuni.2007.09.010

Hsieh, C.S., Y. Liang, A.J. Tyznik, S.G. Self, D. Liggitt, and A.Y. Rudensky. 2004. Recognition of the peripheral self by naturally arising CD25+ CD4+ T cell receptors. *Immunity*. 21:267–277. http://dx.doi.org/10.1016/j.immuni.2004.07.009

Huter, E.N., G.A. Punkosdy, D.D. Glass, L.I. Cheng, J.M. Ward, and E.M. Shevach. 2008. TGF-beta-induced Foxp3+ regulatory T cells rescue scurfy mice. *Eur. J. Immunol*. 38:1814–1821. http://dx.doi.org/10.1002/eji.200838346

Larkin, J. III, A.L. Rankin, C.C. Picca, M.P. Riley, S.A. Jenks, A.J. Sant, and A.J. Caton. 2008. CD4+CD25+ regulatory T cell repertoire formation shaped by differential presentation of peptides from a self-antigen. *J. Immunol*. 180:2149–2157.

Leung, M.W., S. Shen, and J.J. Lafaille. 2009. TCR-dependent differentiation of thymic Foxp3$^+$ cells is limited to small clonal sizes. *J. Exp. Med*. 206:2121–2130. http://dx.doi.org/10.1084/jem.20091033

Louvet, C., B.G. Kabre, D.W. Davini, N. Martinier, M.A. Su, J.J. DeVoss, W.L. Rosenthal, M.S. Anderson, H. Bour-Jordan, and J.A. Bluestone. 2009. A novel myelin P0-specific T cell receptor transgenic mouse develops a fulminant autoimmune peripheral neuropathy. *J. Exp. Med.* 206:507–514. http://dx.doi.org/10.1084/jem.20082113

Milpied, P., A. Renand, J. Bruneau, D.A. Mendes-da-Cruz, S. Jacquelin, V. Asnafi, M.T. Rubio, E. MacIntyre, Y. Lepelletier, and O. Hermine. 2009. Neuropilin-1 is not a marker of human Foxp3+ T reg. *Eur. J. Immunol.* 39:1466–1471. http://dx.doi.org/10.1002/eji.200839040

Miyao, T., S. Floess, R. Setoguchi, H. Luche, H.J. Fehling, H. Waldmann, J. Huehn, and S. Hori. 2012. Plasticity of Foxp3(+) T cells reflects promiscuous Foxp3 expression in conventional T cells but not reprogramming of regulatory T cells. *Immunity.* 36:262–275. http://dx.doi.org/10.1016/j.immuni.2011.12.012

Mottet, C., H.H. Uhlig, and F. Powrie. 2003. Cutting edge: cure of colitis by CD4+CD25+ regulatory T cells. *J. Immunol.* 170:3939–3943.

Mucida, D., N. Kutchukhidze, A. Erazo, M. Russo, J.J. Lafaille, and M.A. Curotto de Lafaille. 2005. Oral tolerance in the absence of naturally occurring T regs. *J. Clin. Invest.* 115:1923–1933. http://dx.doi.org/10.1172/JCI24487

Pacholczyk, R., H. Ignatowicz, P. Kraj, and L. Ignatowicz. 2006. Origin and T cell receptor diversity of Foxp3+CD4+CD25+ T cells. *Immunity.* 25:249–259. http://dx.doi.org/10.1016/j.immuni.2006.05.016

Polansky, J.K., K. Kretschmer, J. Freyer, S. Floess, A. Garbe, U. Baron, S. Olek, A. Hamann, H. von Boehmer, and J. Huehn. 2008. DNA methylation controls Foxp3 gene expression. *Eur. J. Immunol.* 38:1654–1663. http://dx.doi.org/10.1002/eji.200838105

Sarris, M., K.G. Andersen, F. Randow, L. Mayr, and A.G. Betz. 2008. Neuropilin-1 expression on regulatory T cells enhances their interactions with dendritic cells during antigen recognition. *Immunity.* 28:402–413. http://dx.doi.org/10.1016/j.immuni.2008.01.012

Tang, Q., K.J. Henriksen, M. Bi, E.B. Finger, G. Szot, J. Ye, E.L. Masteller, H. McDevitt, M. Bonyhadi, and J.A. Bluestone. 2004. In vitro–expanded antigen-specific regulatory T cells suppress autoimmune diabetes. *J. Exp. Med.* 199:1455–1465. http://dx.doi.org/10.1084/jem.20040139

Thornton, A.M., P.E. Korty, D.Q. Tran, E.A. Wohlfert, P.E. Murray, Y. Belkaid, and E.M. Shevach. 2010. Expression of Helios, an Ikaros transcription factor family member, differentiates thymic-derived from peripherally induced Foxp3+ T regulatory cells. *J. Immunol.* 184:3433–3441. http://dx.doi.org/10.4049/jimmunol.0904028

Voskuhl, R.R. 1998. Myelin protein expression in lymphoid tissues: implications for peripheral tolerance. *Immunol. Rev.* 164:81–92. http://dx.doi.org/10.1111/j.1600-065X.1998.tb01210.x

Wang, Q., L. Malherbe, D. Zhang, K. Zingler, N. Glaichenhaus, and N. Killeen. 2001. CD4 promotes breadth in the TCR repertoire. *J. Immunol.* 167:4311–4320.

Wong, J., R. Obst, M. Correia-Neves, G. Losyev, D. Mathis, and C. Benoist. 2007. Adaptation of TCR repertoires to self-peptides in regulatory and nonregulatory CD4+ T cells. *J. Immunol.* 178:7032–7041.

Zhou, X., S.L. Bailey-Bucktrout, L.T. Jeker, C. Penaranda, M. Martínez-Llordella, M. Ashby, M. Nakayama, W. Rosenthal, and J.A. Bluestone. 2009. Instability of the transcription factor Foxp3 leads to the generation of pathogenic memory T cells in vivo. *Nat. Immunol.* 10:1000–1007. http://dx.doi.org/10.1038/ni.1774